AIAA 2013-3956

Performance Analysis of an Integrated Multi-Mode Chemical Monopropellant Inductive Plasma Thruster

Steven P. Berg[1] and Joshua L. Rovey[2]
Missouri University of Science and Technology, Rolla, Missouri 65409

A novel multi-mode spacecraft propulsion concept is presented. The concept combines chemical monopropellant and electric pulsed inductive thruster technology to include shared propellant and shared conical nozzle. Geometry calculations show that existing conical pulsed inductive thruster experiments are typical of large (1000-4000 N) chemical monopropellant thruster nozzles. Performance and propulsion system mass required to accomplish a 1500 m/s delta-V with a 500 kg payload was calculated for geometries including 20-55 degree divergence angles. Results show that combining nozzle geometry is not beneficial in terms of propulsion system mass for small nozzle divergence angles, however using a nozzle with a 55 degree divergence angle results in a 1-2% reduction in propulsion system mass compared to an equivalent thrust system utilizing a separate chemical bell nozzle and flat coil PIT device despite having 19% lower chemical specific impulse and 18% lower electric thrust efficiency. Results suggest that using even larger divergence angles could yield even more benefit.

Nomenclature

A_c	=	combustion chamber cross sectional area
A_t	=	throat area
C	=	capacitance
C_F	=	thrust coefficient
C	=	effective exhaust velocity
c^*	=	characteristic velocity
D_t	=	throat diameter
EP	=	electric propulsion
F	=	thrust
F_{tu}	=	ultimate strength of material
$f(r,z)$	=	current sheet mass distribution function
f_{inert}	=	inert mass fraction
g_0	=	acceleration of gravity
I_1	=	powertrain current
I_2	=	plasma current
I_{sp}	=	specific impulse
L	=	inductance
L_C	=	coil inductance
L_c	=	combustion chamber length
L^*	=	characteristic combustion chamber length, or inductance ratio
M	=	mutual inductance
m	=	current sheet mass
m_{bit}	=	mass bit
m_c	=	combustion chamber mass
m_{cables}	=	mass of electrical cables

[1] Graduate Research Assistant, Aerospace Plasma Laboratory, Mechanical and Aerospace Engineering, 160 Toomey Hall, 400 W. 13th Street, Student Member AIAA.
[2] Assistant Professor of Aerospace Engineering, Mechanical and Aerospace Engineering, 292D Toomey Hall, 400 W. 13th Street, Senior Member AIAA.

m_{inert} = inert mass
m_{pay} = payload mass
m_{PPU} = mass of power processing unit
m_{prop} = propellant mass
m_{sa} = mass of solar array
N = PIT nozzle angle scaling parameter
P_b = burst pressure
P_c = chamber pressure
P_e = nozzle exit pressure
R_e = external circuit resistance
R_p = plasma resistance
r = radial position of current sheet
r_c = combustion chamber radius
$r_{coil.}$ = coil radius
r_t = throat radius
t = time
t_w = wall thickness
V = voltage
v_r = radial current sheet velocity
v_z = axial current sheet velocity
z = axial position of current sheet
α = nozzle divergence half-cone angle
α_r = radial dynamic impedance parameter
α_z = axial dynamic impedance parameter
ΔV = velocity increment
ε = nozzle expansion ratio
η_t = thrust efficiency
θ_c = convergent section angle
γ = specific heat ratio
λ = nozzle divergence correction factor
φ_{tank} = empirical tank sizing parameter
ψ_1 = powertrain critical resistance ratio
ψ_2 = plasma critical resistance ratio
ρ = current sheet density
ρ_{prop} = propellant density
ρ_w = wall material density

superscript
$*$ = nondimensionalized quantity
subscript
0 = initial quantity

I. Introduction

MULTI-mode spacecraft propulsion is the utilization of a combination of high-thrust chemical and low-thrust, high-specific impulse electrical thrusters on a single spacecraft, specifically making use of common propellants and/or integrated hardware. The main benefit of this type of propulsion system is increased mission flexibility since either mode can be utilized at any given time during a mission, whilst still resulting in complete utilization of available propellant. This study introduces and analyzes the potential benefits of a new multi-mode propulsion system concept: a chemical monopropellant thruster and electrical pulsed inductive thruster (PIT) with both shared propellants and hardware.

As previously stated, the main driver for much of the previous research in multi-mode propulsion is the potential to increase spacecraft mission flexibility through the availability of both traditional chemical high-thrust, low-specific impulse and electrical low-thrust, high specific impulse maneuvers.[1,2] This technology has the potential to allow for changes to the satellite mission as needs arise, and could further enable the ability to launch a satellite without necessarily determining a strict mission plan beforehand. Additionally, it has been shown that under certain

mission scenarios it is beneficial in terms of spacecraft mass savings, or deliverable payload, to utilize two separate propulsion systems, even if there is no common hardware or propellant.[3-8] For example, use of a separate chemical rocket to escape earth gravity avoids a long spiral trajectory characteristic of an electric burn, while a high-specific impulse electric burn in interplanetary space saves propellant mass over a chemical rocket.[7] However, it has been shown that even greater mass savings can potentially be realized through the use of shared propellants[9-11] or shared hardware.[12] The overidding question, however, when assessing multi-mode propulsion system performance is whether inherent thruster performance losses accrued as a compromise in integrating either propellant or hardware outweigh the anticipated benefits.

The chemical mode of the concept presented in this paper utilizes a traditional monopropellant thruster. Typically a single chemical propellant, or premixed solution of fuel and oxidizer, is injected onto a catalyst material, which initiates an exothermic decomposition into gaseous products, and is in turn accelerated through a nozzle via gasdynamic expansion to generate thrust. Typical monopropellant thrusters range from mN thrust levels to roughly 2500 N with a specific impulse around 250 seconds. After 2500 N the associated hardware cost, most notably the size of the catalyst bed, outweighs the equivalently capable bipropellant thruster.[13] The workhorse monopropellant for basically the entirety of spaceflight to date has been hydrazine because it is storable and easily decomposed via catalyst to give good propulsion performance.[13] However, because hydrazine is also highly toxic, recent efforts have focused on finding a suitable non-toxic, higher performance replacement.[14-20]

The electric mode of the multi-mode concept presented in this paper is a pulsed inductive plasma thruster (PIT). A PIT device are a high-power electric propulsion thruster in which energy is capacitively stored and then discharged through an inductive coil. The discharge ionizes gaseous propellant near the coil, which generates a current sheet that is subsequently accelerated via Lorentz force to generate high exhaust velocities. Typical thrust values range from the mN regime to roughly 1 N with achievable specific impulses in excess of 3000 seconds.[21] PIT devices have a distict advantage over other electric thruster concepts because they are electrodeless, meaning they do not have lifetime or contamination issues associated with electrode erosion. As will become apparent in the analysis presented in this paper, this is essential to this multi-mode concept since the PIT device can be operated with a wide range of propellants, including those found in typical monopropellant exhaust species such as CO_2, H_2O, and NH_3.[21,22] While most of the initial research on PIT devices focused on planar coils,[23] recent investigations have included conical inductive coils.[24-29] The main benefit of using a conical coil as opposed to a planar coil is thought to be better propellant mass utilization, and thus potentially increased overall efficiency, despite the addition of a radial component to the Lorentz force that does not benefit the device efficiency.[28]

The following sections present a novel multi-mode propulsion concept, and attempt to quantify and analyze its potential benefits. Section II presents the high-level view of the overall concept. Section III describes the theoretical methods that will be used to analyze the concept. Section IV presents the results, and Section V the following discussion. Finally, Section VI highlights the main conclusions of the work.

II. Concept Overview

The concept presented in this paper is a novel multi-mode spacecraft propulsion system that incorporates both shared propellant and hardware. In essence, the system makes use of common propellant, tanks, lines, and nozzle geometry to function as either a chemical monopropellant thruster or electric pulsed inductive thruster on demand. The following paragraphs describe the system at the conceptual level and outline the design issues and potential solutions that will become the subject of further inquiry.

An illustration of the concept is shown in Fig. 1. As stated, both monopropellant and PIT thrusters operate using the same conical nozzle geometry in addition to shared propellant and tank lines. The propellant shown in hydrazine, but could be virtually any monopropellant, as will be discussed in a later section. In chemical propulsion (CP) mode, the propellant flow rate is high enough that catalytic decomposition results in high temperature high pressure gas that expands out the nozzle. In electric propulsion (EP) mode, the propellant flow rate is much lower such that catalytic decomposition results in a low density ambient gas that slowly diffuses out the nozzle. The low density gas is then ionized and accelerated by a pulsed inductive coil embedded in the thruster nozzle. The main difference between this concept and a conventional monopropellant thruster is the addition of a ceramic portion of the nozzle to accommodate the EP operation.

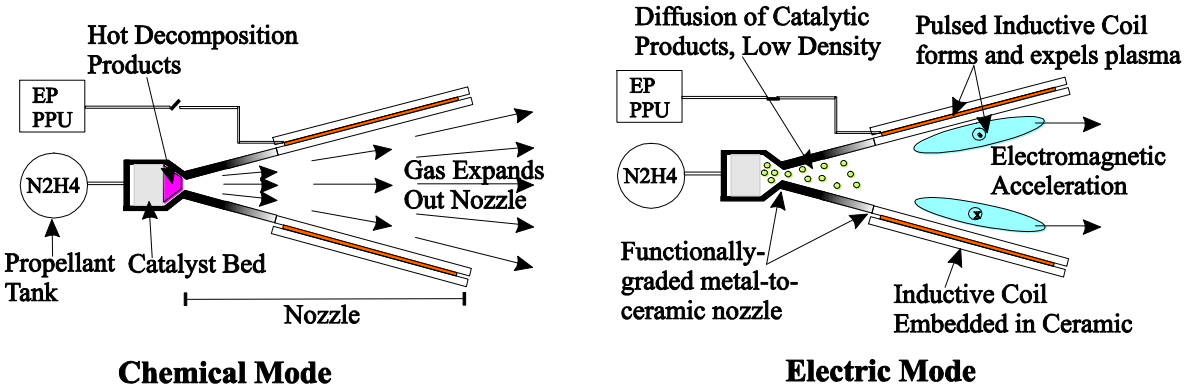

Figure 1. Illustration of the Multi-Mode Concept. *Illustration of the thruster in chemical and electric mode of operation. The thruster operates with the same propellant and nozzle geometry in both modes.*

The most prevalent questions regarding the implementation of this concept, or any multi-mode concept, is whether it is actually possible to integrate components, and then whether it is even advantageous to do so. This concept requires the propellant as well as the nozzle to function in both modes. As mentioned, PIT devices have the distict advantage of being electrodeless, and therefore can conceivably function well with any gaseous species, including monopropellant exhaust. PIT devices have already demonstrated performance with hydrazine exhaust products ammonia and nitrogen.[21] Ammonia propellant even showed improved performance due to less radiative losses.[21,22] The biggest issue with regards to the propellant then is the decomposition, and subsequent diffusion into the nozzle during PIT operation. Figure 1 shows that the catalyst bed designed for chemical mode operation might be used for electric mode operation where a much lower propellant flow rate is introduced into the catalyst bed, then the exhaust products diffuse into the nozzle chamber. However, this, while being the most simple configuration, is likely unsuitable given the fact that the current sheet in PIT operation is formed best when the neutral propellant is located as close to the wall as possible.[30] Furthermore, since current sheet formation has been a major issue in recent PIT designs,[29,31] it is likely that a separate gas generator and injector will be required.

The second major question that needs to be addressed is the nozzle itself. As mentioned, the nozzle must include a ceramic, or other dielectric material, in order to accommodate the PIT thruster operation mode. This is necessary because the PIT coil must be electrically isolated from the propellant in order to induce ionization and acceleration. Typically, chemical nozzles are not made of ceramic material because the temperature gradients during operation are too high for ceramic material to remain structurally sound. One solution to this issue may be to employ state-of-the-art additive manufacturing technology. Specifically, Freeze-form Extrusion Fabrication (FEF) has demonstrated the ability to create functionally graded metal-to-ceramic material in shapes such as cones or other aerospace-related parts, such as in hypersonic vehicles.[32-34] This type of nozzle is illustrated in Figure 1.

While the two aforementioned questions remain as technical hardware issues, the most basic question with regards to this concept is, given expected losses in performance, does it make sense to integrate this system, or would it be better served as a separate system, utilizing separate nozzles for either mode which would perform at state-of-the-art. A typical chemical nozzle is not a cone, but rather a bell, which results in a smaller angle at the exit ($<5^o$ typically), that yields a more axial exit velocity profile, and therefore more efficient thrust generation resulting in a higher specific impulse. When a cone is used, it is typically a 15^o half cone angle. In contrast, the most efficient PIT geometry, aside from neutral propellant utilization considerations, is actually a flat coil, or equivalently a cone with a 90^o divergence half angle since it results in a completely axial Lorentz force acceleration on the ionized propellant.[28] As the divergence angle is decreased, a radial body force results that compresses the plasma and yields little benefit in terms of thrust generation.[27] Integrating the nozzle, therefore, introduces performance losses in at least one mode of the two compared to the 'ideal' performance of each mode separately. The question is then whether the mass savings gained by using one nozzle outweighs the extra propellant mass required due to the performance loss. Analysis in this paper will focus on the answer to this question.

III. Performance Models and Systems Considerations

This section describes the models used to assess the performance of the proposed system operating in either chemical or electric mode, as well as the preliminary system sizing assumptions that will be the basis for the

analysis of the propulsion system as a whole. This analysis will include systems representative of the integrated geometry of Fig. 1 as compared to separate state-of-the-art thrusters; more specifically, a system consisting of a bell nozzle for the chemical mode and a separate flat coil (90^o conical half angle) for the electric mode. The propellant chosen for the entirety of the following analyses is hydrazine. Because ammonia, a main decomposition product of hydrazine, outperforms xenon or other noble gases in the PIT mode, it is inevitable that this type of system will benefit from simply integrating the propellant for use in both modes if hydrazine is chosen as the propellant. However, the main reason in focusing on hydrazine for this study is that not enough is known about the plasma properties of the monopropellant exhause species of advanced monopropellants to make a reasonable performance assessment. This will be addressed further when discussing the PIT model assumptions.

A. Chemical Mode Performance and Sizing

The propellant selected for the preliminary studies presented in this paper is hydrazine. Depending on the geometry of the catalyst bed, the decomposition can be tuned to yield a wide variety of combustion temperatures and exhaust products, and therefore performance, depending on the degree of ammonia dissociation.[35] Designing for little or no ammonia dissociation yields the highest performance, but this is impractical since the resulting combustion temperature reduces the catalyst bed lifetime.[13] A typical design value is to allow for roughly 40% ammonia dissociation. This gives a combustion temperature of 1350 K, a specific heat ratio of 1.23, and a characteristic velocity of 1345 m/s.[36] These values will be used for all subsequent chemical performance and thruster sizing calculations.

Given the aforementioned combustion characteristics of the propellant, a chemical thruster at a desired thrust level can be sized by specifying three additional parameters: chamber pressure, nozzle expansion ratio, and divergence half-cone angle. The nozzle throat area is calculated from Eq. (1),

$$A_t = \frac{F}{C_F P_C}, \tag{1}$$

where the thrust coefficient is given by Eq. (2),

$$C_F = \lambda \sqrt{\frac{2\gamma}{\gamma-1}\left(\frac{2}{\gamma+1}\right)^{\frac{\gamma+1}{\gamma-1}}\left[1-\left(\frac{P_e}{P_c}\right)^{\frac{\gamma-1}{\gamma}}\right]} + \frac{P_e}{P_c}\varepsilon, \tag{2}$$

and the pressure ratio can be solved iteratively using Eq. (3),

$$\frac{1}{\varepsilon} = \left(\frac{\gamma+1}{2}\right)^{\frac{1}{\gamma-1}}\left(\frac{P_e}{P_c}\right)^{\frac{1}{\gamma}}\sqrt{\left(\frac{\gamma+1}{\gamma-1}\right)\left(1-\frac{P_e}{P_c}\right)^{\frac{\gamma-1}{\gamma}}}. \tag{3}$$

Because the goal of the paper is to essentially assess the effect of non-ideal performance on the overall multi-mode system, the divergence correction factor has been added to the thrust coefficient calculation, shown in Eq. (4),

$$\lambda = \frac{1}{2}\left(1+\cos(\alpha)\right), \tag{4}$$

which has been shown experimentally to be reasonably accurate for half-cone angles of up to 45^o.[37] The specific impulse can then be calculated from Eq. (5),

$$I_{sp} = \frac{C_F c^*}{g_0}. \tag{5}$$

Given the specified parameters, and calculations from Eqs. (1)-(4), the remaining geometry of the divergence section, namely exit area and length are calculated through simple trigonometric relations. The thrust chamber geometry can be calculated through empirical means by Eqs. (6) and (7),[38]

$$A_c = A_t\left(8D_t^{-0.6}+1.25\right) \tag{6}$$

$$L_c = L^* \frac{A_t}{A_c}, \tag{7}$$

where the characteristic length, L^*, historically falls between 0.5 and 2.5, with monopropellant thrusters having characteristic lengths in the high end of this range. Therefore, a characteristic length of 2.5 is chosen for purposes of

this analysis. Since all of the geometric parameters of the thruster have been calculated, the mass can be estimated by the following equations. The wall thickness is estimated by Eq. (8),

$$t_w = \frac{P_b D_c}{2F_{tu}} \tag{8}$$

and the mass of the thrust chamber is subsequently calculated using Eq. (9),

$$m_c = \pi \rho_w t_w \left[2r_c L_c + \frac{r_c^{\,2} - r_t^{\,2}}{\tan\theta_c} \right]. \tag{9}$$

For the preliminary calculations, the burst pressure is assumed to be twice the chamber pressure and the material is assumed to be columbium (F_{tu}=*310 MPa,* ρ_w=*8600 kg/m*^{3}), a generic thrust chamber material. Additionally, the angle of the convergence section is assumed to be 45^o in all cases, recognizing that it typically comprises only a small percentage of the total thruster mass.

B. Electric Mode Performance Model

The model used to calculate performance in the electric pulsed inductive thruster mode is based on a circuit model that includes the power train coupled inductively to the plasma. The circuit equations are coupled to the momentum equation to describe the acceleration of the plasma and elucidate performance.[23] In this study, the non-dimensionalized equations[39] are employed initially to gauge performance trends independent of powertrain and plasma properties. Furthermore, the two-dimensional momemtum equation based on the insights of Hallock et. al.[24,27,28] is used in order to estimate the performance losses by utilizing a conical coil as opposed to a flat coil. The equations are summarized here, and the reader is referred to the literature cited above for a more rigorous development.

The non-dimensionalized circuit equations governing the powertrain portion of the circuit are given in Eqs. (10)-(12),

$$\frac{dI_1^*}{dt^*} = \frac{L^* V^* + (M^* I_1^* + I_2^*)\left(\frac{dM^*}{dt^*}\right) - I_2^* M^* L^* \psi_2 - I_1^* L^* \psi_1}{(L^* + 1) - (M^*)^2} \tag{10}$$

$$\frac{dI_2^*}{dt^*} = M^* \frac{dI_1^*}{dt^*} + I_1^* \frac{dM^*}{dt^*} - I_2^* L^* \psi_2 \tag{11}$$

$$\frac{dV^*}{dt^*} = -I_1^*. \tag{12}$$

The time derivative of mutual inductance, accounting for both axial and radial motion of the plasma, in non-dimentional form is Eq. (13),

$$\frac{dM^*}{dt^*} = \frac{N}{2}\left(r^*\right)^{\frac{N}{2}-1} \frac{dr^*}{dt^*} \exp\left(-\frac{z^*}{2}\right) - \frac{1}{2}\left(r^*\right)^{\frac{N}{2}} \exp\left(-\frac{z^*}{2}\right) \frac{dz^*}{dt^*}, \tag{13}$$

where *N* is essentially a fitting parameter for the mutual inductance of conical coils found in Ref. 37. The geometric significance of this parameter will be investigated in a later section. The non-dimensional form of the acceleration in the axial and radial direction is Eq. (14) and (15), respectively,

$$\frac{dv_z^*}{dt^*} = \left(\alpha_z (I_1^*)^2 \exp\left(-z^*\right)(r^*)^N\right) / m^* \tag{14}$$

$$\frac{dv_r^*}{dt^*} = \left(-\alpha_r N (I_1^*)^2 \exp(-z^*)(r^*)^{N-1}\right) / m^*, \tag{15}$$

where the velocity components are simply

$$\frac{dz^*}{dt^*} = v_z^* \tag{16}$$

$$\frac{dr^*}{dt^*} = v_r^*. \tag{17}$$

Finally, the mass accumulation by the current sheet can be calculated via the snowplow model, Eq. (18),

$$\frac{dm^*}{dt^*} = \rho^* f(r^*, z^*) v_z^*. \tag{18}$$

Eqs. (10)-(18) represent a system of coupled first-order ODEs that can be solved readily with the Runge-Kutta method combined with the following initial conditions:

$$\begin{gathered} I_1^* = I_2^* = z^* = v_z^* = v_r^* = 0 \\ V^* = M^* = r^* = 1 \\ m^* = \frac{m_0}{m_{bit}} \end{gathered} \tag{19}$$

The non-dimensionalized variables are expressed in dimensional quantities by the following:[39]

$$\begin{gathered} I_1^* = \frac{1}{V_0}\sqrt{\frac{L_0}{C}} I_1 \\ I_2^* = \frac{1}{V_0}\sqrt{\frac{L_0}{C}} I_2 \\ t^* = \frac{t}{\sqrt{L_0 C}} \\ z^* = \frac{z}{z_0} \\ V^* = \frac{V}{V_0} \\ M^* = \frac{M}{L_C} \\ v_z^* = \frac{\sqrt{L_0 C}}{z_0} v_z \end{gathered} \tag{20}$$

The non-dimensionalized radial components of current sheet position and velocity are given by Eq. (21),

$$\begin{gathered} r^* = \frac{\bar{r}}{\bar{r}_{coil}} \\ v_r^* = \frac{\sqrt{L_0 C}}{\bar{r}_{coil}} v_r \end{gathered} \tag{21}$$

The scaling parameters that appear in Eqs. (10)-(18) are[39]

$$\begin{gathered} L^* = \frac{L_0}{L_C} \\ \psi_1 = R_e\sqrt{\frac{C}{L_0}} \\ \psi_2 = R_p\sqrt{\frac{C}{L_0}} \\ \alpha_z = \frac{C^2 V_0^2 L_C}{2 m_{bit} z_0^2} \end{gathered} \tag{22}$$

and a radial component of the dynamic impedance parameter introduced as a consequence of the two-dimensional acceleration is[24]

$$\alpha_r = \frac{C^2 V_0^2 L_C}{2 m_{bit} \bar{r}_{coil}^2} \tag{23}$$

Finally, the main performance metrics for the electric mode, efficiency and specific impulse can be calculated from Eqs. (24) and (25), repectively, as

$$\eta_t = \frac{m^* v_z^*}{2 L^* \alpha_z} \tag{25}$$

$$I_{sp} = \frac{c}{g_0} \tag{26}$$

where the exhaust velocity is the axial velocity, v_z, at the exit of the accelerator. It should be highlighted that using the non-dimensional form of the governing equations allows the calculation of the performance metrics in Eqs. (25) and (26) by only specifying parameters for the coil geometry, coil inductance, mass bit, and powertrain capacitance and voltage thereby allowing discussion of the performance of the geometry independent of the plasma properties of the propellant. In reality, these parameters will be affected by propellant choice, and efforts have been made to include the energy equation in the model to examine the effects.[40] However, because the plasma properties of various propellants, namely exhaust from various monopropellants, is unknown, it is beyond the scope of this study to include these effects. Finally, the specific impulse and efficiency calculated from Eqs. (25) and (26) can be used to determine the thrust of the PIT device for a given input power, Eq. (27),

$$\eta_t P_{thr} = \frac{1}{2} F I_{sp} g_0 \tag{27}$$

C. Propulsion System Sizing

The majority of the propulsion system sizing conducted in this study is based on empirical baseline design estimates outlined in Humble.[38] The mass of propellant required to accelerate a spacecraft through a desired velocity change can be calculated from the rocket equation, Eq. (28),

$$m_{prop} = \frac{m_{pay}\left(\exp\left(\frac{\Delta V}{I_{sp} g_0}\right) - 1\right)\left(1 - f_{inert}\right)}{1 - f_{inert}\exp\left(\frac{\Delta V}{I_{sp} g_0}\right)} \tag{28}$$

where the inert mass fraction is given by Eq. (29),

$$f_{inert} = \frac{m_{inert}}{m_{prop} + m_{inert}} \tag{29}$$

and the inert mass is composed of the thruster, propellant feed lines and valves, propellant and pressurant tanks, power processing unit (PPU), and structural mounts for the propulsion system. The mass of the tanks can be estimated empirically by Eq. (30),

$$m_{\tan k} = \frac{P_b m_{prop} \rho_{prop}}{g_0 \phi_{\tan k}} \tag{30}$$

where the burst pressure is again assumed to be twice the tank pressure, which is chosen to be 300 psi plus a 20% injector head loss and 0.35 psi overall line losses for the propellant tanks and 1450 psi for helium pressurant tanks. Also, the empirical tank sizing parameter is chosen to be 2500 m for the propellant tank, and 6350 m for the helium tanks. These values correspond to typical stainless steel (compatible with hydrazine[41]) and titanium tank material, respectively. Since the volume of the pressurant tank is not known beforehand, the pressurant required must be solved for iteratively until the mass of pressurant is sufficient to occupy both pressurant and propellant tanks at the desired propellant tank pressure. The mass of lines and valves is estimated as 50% of the thruster mass, a value typical of monopropellant thrusters historically. Finally, the mass of structural mounts is assumed to be 10% of the total inert mass. Eq. (27) is then solved iteratively for the propellant mass.

In terms of the electric mode of propulsion, the mass of the power processing unit (PPU), associated cables and switches, as well as the powertrain components of the electric thruster itself will have a substantial effect on the

overall propulsion system mass. Hofer and Randolph have developed empirical relations to estimate the mass of the PPU, associated cables, as well as the solar array for high-power electric propulsion technologies, including the PIT.[42] These estimates are given in Eqs. (31)-(33),

$$m_{ppu} = 1.7419 P_{thr} + 4.654 \tag{31}$$

$$m_{cables} = 0.06778 P_{thr} + 0.7301 \tag{32}$$

$$m_{sa} = 3 P_{thr} \tag{33}$$

with power in kW and mass in kg. The mass of the electrical components of the thruster itself is more difficult to estimate because, to date, only a limited number of pulsed inductive thrusters have been studied and there has been little work done on optimizing these components. However, attempts to develop a flight version of the FARAD thruster provide some insight at least to the relartive scale of these components.[43,44] For a Bernardes & Merryman pulsed powertrain, the total mass of the electrical components was 29.1 kg. This includes the capacitor bank, pre-ionization antenna and cabling, switches, bus work, diodes, and coaxial cables. Additionally, this configuration was deemed adequate to produce 100 J/pulse at up to 40 kW continuous power. As will be shown in the results section, this is well within the range of interest for the geometries in this study. Therefore, a constant 29.1 kg will be assumed for the PIT electrical components in all systems hereafter.

IV. Results

The main results of the analysis methods described above are presented below. First, chemical and electrical performance are computed separately in order to determine useful trends to apply to the combined analysis. For the combined system analysis, three geometries are selected for study. These include a 20^o, 38^o, and 55^o nozzle geometry, of which the requisite electromagnetic properties of the PIT coil have been determined in previous studies.[27,28,45] As will be shown, these encompass a sufficient selection to draw relevant conclusions for a multi-mode monopropellant/PIT system.

A. Chemical Thruster Sizing

With the assumptions stated in Section III.a., thruster nozzle geometry is calculated for chemical thrust levels up to 2500 N, which, as stated, is near the top end for monopropellant thrusters. Fig. 2 shows the percent mass savings gained by using an integrated nozzle, as proposed, as opposed to separate nozzles for both modes. This includes the thrust chamber and nozzle only. Also note that in this figure the same conical geometry has been assumed for both modes, i.e. the integrated system is compared to an equivalent separate system of two divergent section nozzles. Fig. 2 therefore indicates an upper bound on the potential mass savings by integrating the nozzle on the thruster. Two important trends can also be commented upon. The mass savings does not grow significantly after 500 N in any case and the percent savings only increases by roughly 2 percent for an expansion ratio of 200 compared to 50. For simplification then, the expansion ratio will be limited to 200 herein because, as will be shown, this will encompass the most relevant geometry for the electric mode. However, the full thrust range shown in Fig. 2 will be considered since PIT performance is highly dependent on geometry according to the model outlined previously.

In order to guage the relevance of the size of the thrusters with typical monopropellant thrust levels in comparison to anticipated conical PIT geometry, the throat and exit diameter, as well as nozzle length is computed and shown in Fig. 3. From the figure, it is easily seen that divergence half-cone angle makes little difference on the throat and exit diameters. There is a slight increase as half-cone angle increases due to the need for a larger throat area to process larger mass flow to achieve the same thrust. The main difference, however, is length, which increases by more than double for 15^o compared to 45^o. However, the important consideration here is how these values compare to current PIT technology. The conical PIT thrusters under investigation had an inner diameter of 8 cm and a length of 10 cm at half-cone angles of 20 and 38 degrees.[27] This corresponds to an equivalent chemical thruster size of at least 1000 N and 2500 N, respectively. So, the current conical PIT technology being investigated corresponds to nozzles in the typical monopropellant thrust range, although there is no fundamental reason why the PIT geometry could be larger or smaller, to some extent.

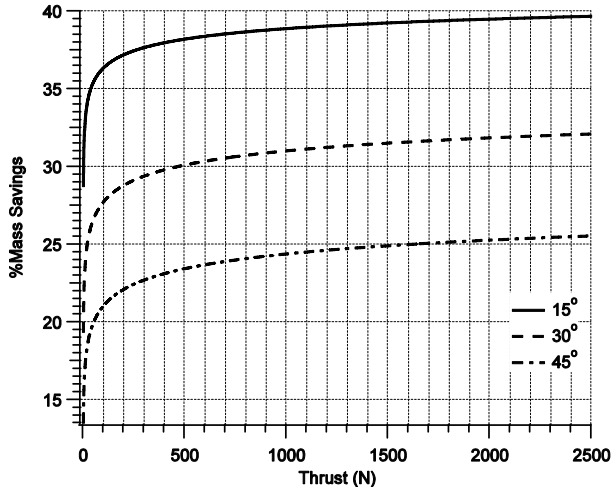

a)

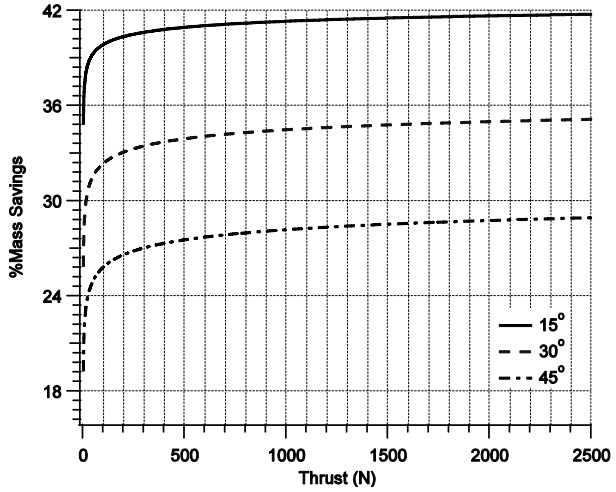

b)

Figure 2. Integrated Nozzle Mass Savings (Thruster Only). *Percent mass saved by integrating nozzle geometry over an equivalent multi-mode system using separate nozzles for expansion ratios of a) 50 and b) 200 and for divergence half-cone angles of 15, 20, and 45 degrees.*

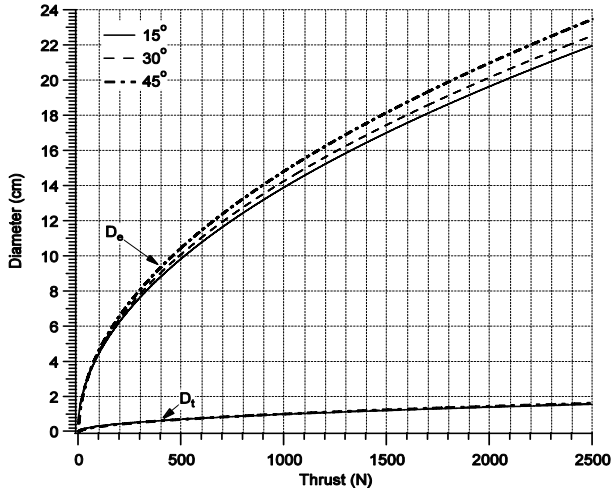

a)

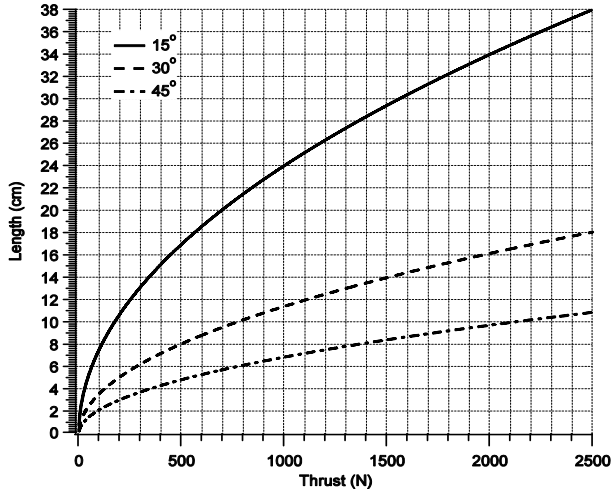

b)

Figure 3. Physical Dimensions of Thruster. *a) Diameters and b) length of thruster nozzle divergent sections at half-cone angles of 15, 30, and 45 degrees.*

B. PIT Performance

The nondimensionalized PIT performance is investigated initially following the model and assumptions outlined in Section III.b. Fig. 4 shows the thruster efficiency as a function of the radial dynamic impedance parameter. The assumed values not shown in the figure are the following: the critical resistance ratios ($\psi_1=\psi_2=1$), the inductance ratio ($L^*=0.121$), and the axial dynamic impedance parameter ($\alpha_z=2.1$). The values chosen correspond to near optimum for planar pulsed inductive devices.[39] The actual physical significance of the divergence parameter, N, is unknown to this point; however, qualitatively a small value of N in general corresponds to a divergence angle closer to 90°,[28] and the $N=0$ value gives the solution for a planar device. This can be seen from Eqs. (10)-(18) as setting $N=0$ removes all radial dependence. The physical significance of this parameter will be investigated further, as will be discussed in the future work section. The figure illustrates some important qualitative trends that will be considered as the analysis progresses. The first is that conical PIT thrusters will perform more poorly than planar devices, absent propellant utilization efficiency. While propellant utilization efficiency could actually play a major role in the value of conical PIT devices over planar devices, it has yet to be adequately quantified. For the conical geometries, the efficiency increases as the radial dynamic impedance parameter decreases. From Eq. (23), for

constant power and mass bit, this means that larger radii will effectively raise the efficiency of the thruster, again absent any propellant utilization efficiency effects. Any practical limit on this, however, remains to be identified.

To quantify the performance of an individual thruster geometry, one must specify parameters for the driving circuitry. As was the case in describing the physical mass of the circuitry components, minimal optimization has been conducted into the driving circuitry of PIT thrusters, especially conical PIT thrusters. Qualitatively, the driving circuitry of a conical PIT, as opposed to a flat coil PIT, should have a longer characteristic circuit time since the acceleration of the current sheet is slower due a portion of the Lorentz force acting to compress the plasma rather than accelerate it.[45] For a given geometry, the parameters of the circuitry can be chosen to optimize thruster efficiency for a desired specific impulse. This is shown in Fig. 5. The calculations conducted for this figure assume a parasitic inductance of 100 nH,[45] a powertrain circuitry resistance of 6 mΩ, a plasma resistance of 10 mΩ,[21] and a mass bit of 0.15 mg/pulse.[43] These reflect values used in previous experiments as indicated by the citations, and are relatively representative of the current state-of-the-art. From Fig. 5a, increasing the capacitance of the external circuitry shifts the optimum voltage to lower levels, but the peak efficiency remains relatively constant. Fig. 5b also shows that a wide range of specific impulses are available for a given capacitance by adjusting the initial voltage prior to discharging the circuitry. It is therefore reasonable to assume that the circuitry can effectively be tuned to a design specific impulse, whilst still achieving optimum efficiency.

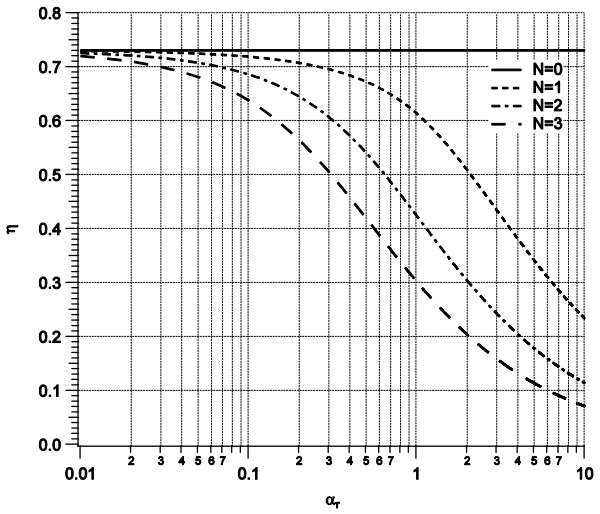

Figure 4. Effect of Divergence Angle and Diameter on Conical PIT Efficiency. *Efficiency as a function of radial dynamic impedance parameter for half-cone divergence parameters of 0-3.*

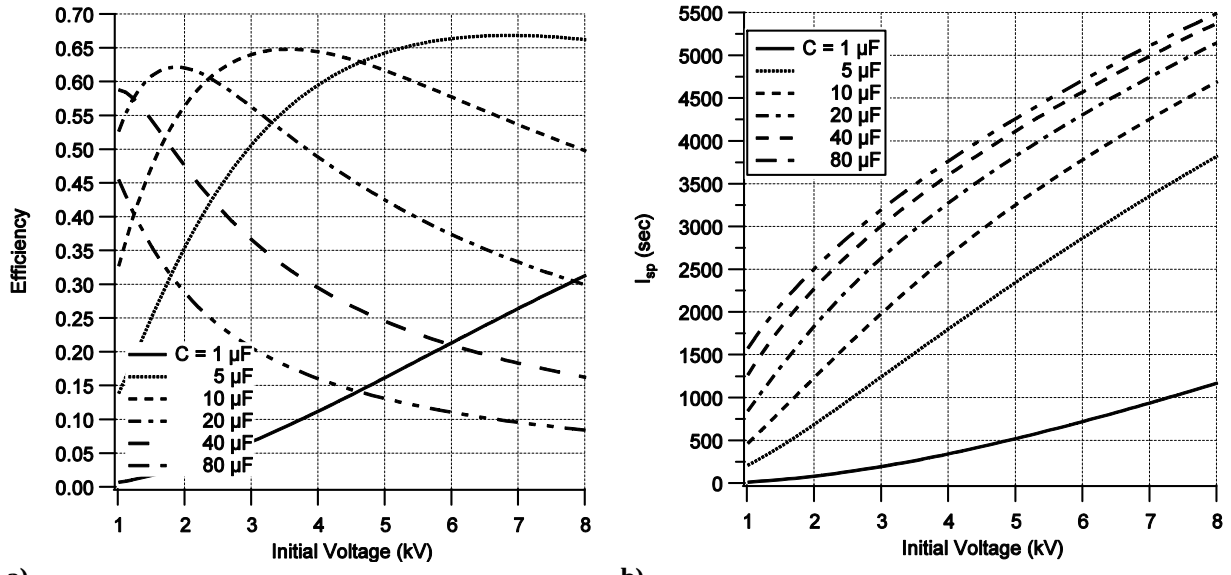

a) **b)**

Figure 5. Effect of Driving Circuitry Parameters on PIT Performance. *a) Efficiency and b) Specific impulse of 90° PIT coil for various capacitance and initial voltages.*

C.) Multi-Mode System Sizing

Six systems are selected for comparison and are summarized in Table 1. These are based on three conical PIT geometries of which enough empirical data was available to make reasonable performance predictions.[27,28,45] Systems are numbered based on the selected conical PIT geometry. Systems with the letter 'I' at the end represent the integrated nozzle systems, while the other systems represent separate, but state-of-the-art thrusters for each mode. For example, System 20I includes the integrated nozzle geometry. The chemical thrust is back calculated based on an expansion ratio of 200. The same thrust is then used for the comparable, unitegrated system denoted as System 20, but with the specific impulse of a bell nozzle. For the PIT performance calculations, a thrust and specific impulse are selected, then power requirements are calculated from Eq. 27. The efficiency of a given coil geometry is calculated by the same methods employed to generate Fig. 5, whereby the capacitance and voltage are chosen such that efficiency is maximized for the chosen specific impulse.

Table 1. Performance of Multi-Mode Systems Selected for Comparison.

System	Chemical	Electric	F_{chem} [N]	$I_{sp,chem}$ [sec]	η_{chem}	F_{elec} [N]	$I_{sp,elec}$ [sec]	η_{elec}	P_{elec} (kW)
20	Bell Nozzle	90° Coil	1430	262	0.99	1	2200	0.68	15.9
20I	20° Conical	20° Coil	1430	259	0.97	1	2200	0.27	40.0
38	Bell Nozzle	90° Coil	3170	262	0.99	1	2200	0.68	15.9
38I	38° Conical	38° Coil	3170	240	0.89	1	2200	0.43	25.1
55	Bell Nozzle	90° Coil	4755	262	0.99	1	2200	0.68	15.9
55I	55° Conical	55° Coil	4755	211	0.79	1	2200	0.50	21.6

The total mass of each propulsion system, as described in Section III.c, is computed for a mission comprising a velocity increment of 1500 m/s with a 500 kg payload. Fig. 6 shows the propulsion system mass as a function of EP fraction, which is the fraction of the total velocity increment conducted using the PIT system. As expected, total propulsion system mass decreases with increased EP fraction since the high specific impulse decreases the required propellant mass as well as tankage and associated structure. Systems involving the 38 and 20 degree integrated nozzles actually require roughly 10% and 30%, repectively, greater propulsion system mass than their unintegrated counterparts due to the decreased chemical performance as well as greater power system mass. However, for EP fractions above 0.2, integrating the nozzle actually decreases propulsion system mass by 1-2% over the separate, ideal nozzle geometries.

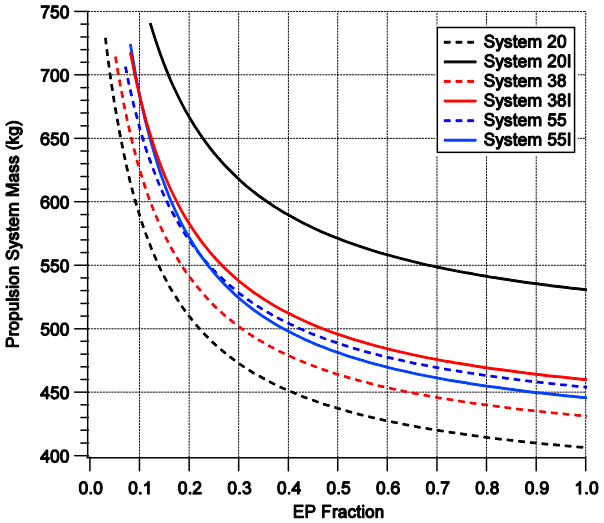

Figure 6. Total Propulsion System Mass. *Mass of all components comprising the propulsion systems described in Table 1 as a function of EP usage.*

Additional conclusions may be drawn by considering systems involving the same power level. The loss in the electric mode is then thrust rather than power system mass. Considering a 30 kW power system, the electric thrust is then 1.9 N for Systems 20, 38, and 55, while the thrust for Systems 20I, 38I, and 55I is 0.75 N, 1.2 N,and 1.4 N, respectively. The total propulsion system mass for the same 1500 m/s velocity increment and 500 kg payload is shown in Fig. 7. All of the integrated systems are less massive than the systems comprising two separate thrusters at all possible EP fractions. Missions with a 500 kg payload undergoing a velocity increment of 1500 m/s with these systems utilizing greater than 90% chemical propulsion mode are not possible due to the exponential nature of the rocket equation. System 55I shows the largest benefit over its unitegrated counterpart, with a 2-7% decreased propulsion system mass with the largest benefit at an EP fraction of unity. Systems 20I and 38I show a 1-2% and a 1-4% decreased system mass, respectively, over their counterparts. However, as mentioned, this comes at a cost of burn time in order to achieve the desired velocity change. This is shown in Fig. 8. System 55I takes roughly 37% longer to complete the velocity change at every EP

fraction compared to System 55, while Systems 38I and 20I take 60% and 160% longer time to achieve the velocity change compared to their counterparts, respectively.

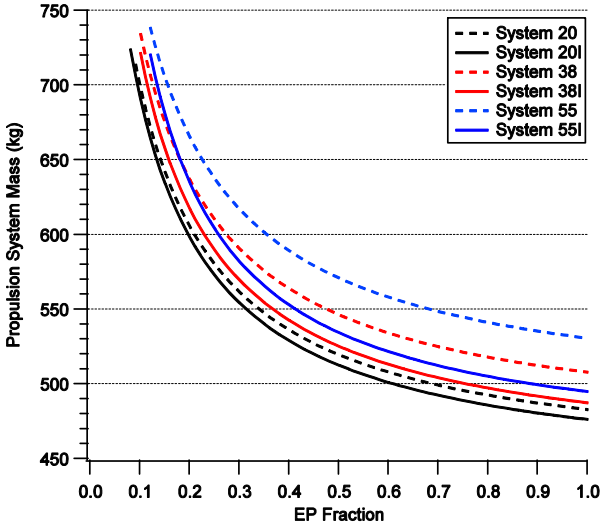

Figure 7. Total Propulsion System Mass for 30 kW Power. *Total mass of all propulsion system components for 30 kW system power as a function of EP usage.*

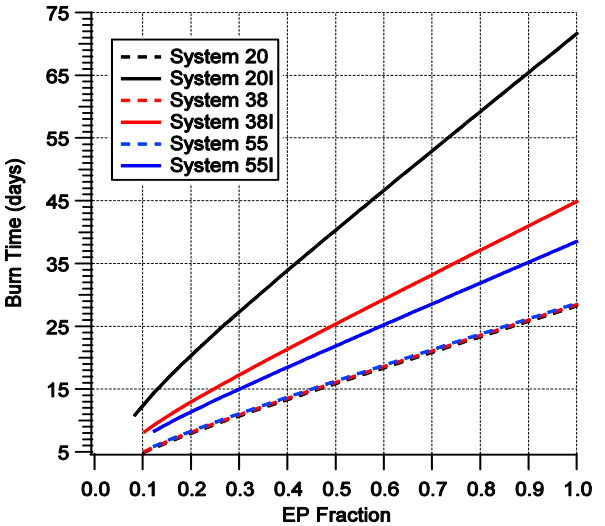

Figure 8. Total Burn Time. *Total burn time to achieve a 1500 m/s velocity increment for all for 30 kW system power as a function of EP usage.*

V. Discussion

The results presented in the previous section show that integrating the nozzle geometry in a multi-mode chemical/PIT system yields, at best, marginal improvements over a system consisting of separate, but state-of-the-art in performance, thruster geometry. However, as will be discussed, due to the relative lack of maturity of PIT technology the assumptions made in this analysis may not lead to a conclusive assessment of the multi-mode prospects of the technology.

As can be reasonably inferred from Figs. 6-8, the performance losses accrued by integrating the geometry result in far greater additional system mass due to additional electric hardware compared to additional propellant needed for the chemical mode. For System 20I, the power system is twice as massive as that for System 20 and equates to 31-43% of its total system mass from EP fractions of 0.1-1.0. By comparison, the propellant for System 55I requires 5% more propellant at the lowest possible EP fraction compared to System 55. The main consideration here is then the electric mode, as evidenced by the fact that the integrated systems with greater cone angles yielded closer to, or smaller system masses than their equivalent, state-of-the-art performance counterparts. It is therefore imperative to discuss the assumptions made in computing electric performance in order to assess the overall multi-mode system. Due to the lack of research on the subject, propellant utilization efficiency in PIT thrusters has been ignored in this study. In fact, adequate quantification of propellant utilization efficiency will lead to even greater benefits than calculated in this study. This is due to the fact that the conical geometry is inherently conducive to better propellant utilization simply the neutral species are likely to be contained closer to the coil than is possible in a 90^{o} coil. And, in fact, this was the original motivation behind studying conical PIT geometries.[26-28] Additionally, this study was limited to just three geometries. Although these comprise an adequate sweep of high-thrust monopropellant thrusters, it may be even more beneficial to consider larger, bipropellant thruster geometry. This is clearly evident in Fig. 4, as increasing the radius of the PIT coil will yield higher efficiency. However, it is not applicable yet to quantitatively speculate on how beneficial this may be since it would also likely effect the propellant utilization efficiency negatively.

Systems involving a single 30 kW power system were also investigated. The results show that if a constant power system is considered, it is always beneficial to integrate the nozzle geometry in terms of mass, but at the cost of increased burn duration. While this may not be an applicable comparison in terms of mission scenario, it could be useful when considering generic, flexible systems in which time is not a critical factor, but rather max delta-V capablility or minimized system mass is a greater concern. Again, however, the nozzles with larger divergence angle

are more beneficial in terms of both mass and burn duration. It may therefore be beneficial to consider even larger divergence angles since the decrease in requisite power system mass will likely outweigh the increase in propellant mass due to chemical mode performance losses.

VI. Conclusions

A multi-mode propulsion concept involving a chemical monopropellant and electric pulsed inductive thruster was investigated. Utilizing the same propellant in both systems will be beneficial regardless of geometric configuration since the decomposition products of hydrazine, the current state-of-the-art monopropellant, actually has the highest performance of all gaseous species that have ever been tested experimentally in PIT devices. The majority of this paper focused on determining if integrating the nozzle geometry of the chemical and PIT thruster is beneficial. This is possible since both chemical and PIT devices can function well with a conical geometry. However, a conical geometry is lower performing in terms of specific impulse in the chemical mode, and also lower performing in terms of thrust efficiency in the electric mode.

Results show that integrating the nozzle geometry of the monopropellant and PIT thruster is not beneficial at small divergence angles, specifically 20-38 degrees. However, past 55 degree divergence angle, benefits can be achieved in terms of lower propulsion system mass to accomplish the same mission as a separate geometry, but state-of-the-art performance system. This is significant because chemical thrusters have never before been considered with divergence angles of roughly 45 degrees, illustrating the unique optimization problems multi-mode systems present. This result is specifically tied to the fact that the increase in requisite power system mass for poorer performing PIT devices is large compared to the increase in propellant mass of poorer performing chemical monopropellant thrusters.

References

[1]Haas, J. M., and Holmes, M. R., "Multi-Mode Propulsion System for the Expansion of Small Satellite Capabilities," NATO, Rept. MP-AVT-171-05, 2010.

[2]Rexius, T., and Holmes, M., "Mission Capability Gains from Multi-Mode Propulsion Thrust Profile Variations for a Plane Change Maneuver," *AIAA Modeling and Simulation Technologies Conference*, AIAA Paper 2011-6431, 2011.

[3]Mailhe, L. M., Heister, S. D., "Design of a Hybrid Chemical/Electric Propulsion Orbital Transfer Vehicle," *Journal of Spacecraft and Rockets*, Vol. 39, No. 1, 2002, pp. 131-139.

[4]Kemble, S., Taylor, M. J., "Mission Design Options for a Small Satellite Mission to Jupiter," *54th International Astronautical Congress of the International Astronautical Federation, the International Academy of Astronautics, and the International Institute of Space Law*, IAC-03-A.3.09, 2003.

[5]Lee, S., Hwang, I., "Hybrid High- and Low-Thrust Optimal Path Planning for Satellite Formation Flying," *AIAA Guidance, Navigation, and Control Conference*, AIAA-2012-5046, 2012.

[6]Kluever, C. A., "Spacecraft Optimization with Combined Chemical-Electric Propulsion," *Journal of Spacecraft and Rockets*, Vol. 32, No. 2, 1994, pp. 378-380.

[7]Gilland, J. H., "Synergistic Use of High and Low Thrust Propulsion Systems for Piloted Missions to Mars," AIAA Paper 1991-2346, 1991.

[8]Kluever, C. A., "Optimal Geostationary Orbit Transfers Using Onboard Chemical-Electric Propulsion," *Journal of Spacecraft and Rockets*, Vol. 49, No. 6, 2012, pp. 1174-1182.

[9]Donius, B. R. and Rovey, J. L., "Ionic Liquid Dual-Mode Spacecraft Propulsion Assessment," *Journal of Spacecraft and Rockets*, Vol. 48, No. 1, 2011, pp. 110-123.

[10]Berg, S. P., and Rovey, J. L., "Assessment of Imidazole-Based Energetic Ionic Liquids as Dual-Mode Spacecraft Propellants," *Journal of Propulsion and Power*, Vol. No. 2012, pp.

[11]Berg, S. P., and Rovey, J. L., "Dual-Mode Propellant Properties and Performance Analysis of Energetic Ionic Liquids," *50th Aerospace Sciences Meeting*, AIAA Paper 2012-0975, 2012.

[12]Cofer, A., Venkattraman, A., and Alexeenko, A., "Microspike Based Chemical/Electric Thruster Concept for Versatile Nanosat Propulsion," *47th AIAA/ASME/SAE/ASEE Joint Propulsion Conference & Exhibit*, AIAA Paper 2011-5921, 2011.

[13]Sutton, G. P., and Biblarz, O., *Rocket Propulsion Elements*, 7th, Wiley, New York, 2001.

[14]Zube, D., Wucherer, E., and Reed, B., "Evaluation of HAN-Based Propellant Blends," *39th AIAA/ASME/SAE/ASEE Joint Propulsion Conference & Exhibit*, AIAA Paper 2003-4643, 2003.

[15]Amariei, D., Courtheoux, L., Rossignol, S., Batonneau, Y., Kappenstein, C., Ford, M., and Pillet, N., "Influence of the Fuel on Thermal and Catalytic Decompositions of Ionic Liquid Monopropellants," *41st AIAA/ASME/SAE/ASEE Joint Propulsion Conference & Exhibit*, AIAA Paper 2005-3980, 2005.

[16]Anflo, K, Gronland, T. A., Bergman, G., Johansson, M., and Nedar, R., "Towards Green Propulsion for Spacecraft with ADN-Based Monopropellants," *38th AIAA/ASME/SAE/ASEE Joint Propulsion Conference & Exhibit*, AIAA Paper 2002-3847, 2002.

[17]Slettenhaar, B., Zevenbergen, J. F., Pasman, H. J., Maree, A. G. M., and Morel, J. L. P. A., "Study on Catalytic Ignition of HNF Based Non Toxic Monopropellants," *39th AIAA/ASME/SAE/ASEE Joint Propulsion Conference & Exhibit*, AIAA Paper 2003-4920, 2003.

[18]Anflo, K, Persson, S., Thormahlen, P., Bergman, G., and Hasanof, T., "Flight Demonstration of ADN-Based Propulsion System on the PRISMA Satellite," *42nd AIAA/ASME/SAE/ASEE Joint Propulsion Conference & Exhibit*, AIAA Paper 2006-5212, 2006.

[19]Masse, R. K., Overly, J. A., Allen, M. Y., Spores, R. A., "A New State-of-the-Art in AF-M315E Thruster Technologies," *48th AIAA/ASME/SAE/ASEE Joint Propulsion Conference & Exhibit*, AIAA Paper 2012-4335, 2012.

[20]Hawkins, T., Brand, A., McKay, M., Drake, G., and Ismail, I. M. K., "Characterization of Reduced Toxicity, High Performance Monopropellants at the U. S. Air Force Research Laboratory," Air Force Research Laboratory, Rept. AFRL-PR-ED-TP-2001-137, 2001.

[21]Polzin, K. A., "Comprehensive Review of Planar Pulsed Inductive Plasma Thruster Research and Technology," *Journal of Propulsion and Power*, Vol. 27, No. 3, 2011, pp. 513-531.

[22]Mikellides, P. G., and Neilly, C., "Modeling and Performance Analysis of the Pulsed Inductive Thruster," *Journal of Propulsion and Power*, Vol. 23, No. 1, 2007, pp. 51-58.

[23]Lovberg, R. H., and Dailey, C. L., "Large Inductive Thruster Performance Measurement," *AIAA Journal*, Vol. 20, No. 7, 1982, pp. 971-977.

[24]Hallock, A. K., and Polzin, K. A., "Computational Validation of a Two-dimensional Semi-empirical Model for Inductive Coupling in a Conical Pulsed Inductive Plasma Thruster," *Joint Army-Navy-NASA-Air Force (JANNAF) 8th MSS / 6th LPS / 5th SPS Meeting*, JANNAF-2011-2197, 2011.

[25]Hallock, A. K., Choueiri, E. Y., and Polzin, K. A., "Current Sheet Formation in a Conical Theta Pinch Faraday Accelerator with Radio-frequency Assisted Discharge," *44th AIAA/ASME/SAE/ASEE Joint Propulsion Conference & Exhibit*, AIAA Paper 2008-5201, 2008.

[26]Hallock, A. K., and Choueiri, E. Y., "Effects of Inductive Coil Geometry in the Conical Theta Pinch Faraday Accelerator with Radio Frequency Assisted Discharge," *45th AIAA/ASME/SAE/ASEE Joint Propulsion Conference & Exhibit*, AIAA Paper 2009-5448, 2009.

[27]Hallock, A. K., Polzin, K. A., Bonds, K. W., and Emsellem, G. D., "Effect of Inductive Coil Geometry and Current Sheet Trajectory of a Conical Theta Pinch Pulsed Inductive Plasma Accelerator," *47th AIAA/ASME/SAE/ASEE Joint Propulsion Conference & Exhibit*, AIAA Paper 2011-6068, 2011.

[28]Hallock, A. K., Polzin, K. A., and Emsellem, G. D., "Two-dimensional Analysis of Conical Pulsed Inductive Plasma Thruster Performance," *32nd International Electric Propulsion Conference*, IEPC-2011-145, 2011.

[29]Hallock, A. K., Polzin, K. A., Kimberlin, A. C., and Perdue, K. A., "Effect of Inductive Coil Geometry on the Operating Characteristics of an Inductive Pulsed Plasma Thruster," *48th AIAA/ASME/SAE/ASEE Joint Propulsion Conference & Exhibit*, AIAA Paper 2012-3928, 2012.

[30]Dailey, C. L., and Lovberg, R. H., "Pulsed Inductive Thruster Component Technology," Rept. AFAL-TR-87-012, 1987.

[31]Polzin, K. A., Rose, M. F., and Miller, R., "Operational Characteristics of a Low-Energy FARAD Thruster," *44th AIAA/ASME/SAE/ASEE Joint Propulsion Conference & Exhibit*, AIAA Paper 2008-5011, 2008.

[32]Zhao, Z., Landers, R. G., and Leu, M. C., "Adaptive-Control of Freeze-form Extrusion Fabrication Processes," *ASME Journal of Manufacturing Science and Engineering*, Vol. 132, No. 6, 2012, pp.

[33]Mason, M. S., Huang, T., Landers, R. G., Leu, M. C., and Hilmas, G. E., "Aqueous-Based Extrusion of High Solids Loading Ceramic Pastes: Process Modeling and Control," *Journal of Materials Processing Technology*, Vol. 209, No. 2009, pp. 2946-2957.

[34]Leu, M. C., Deuser, B. K., Tang, L., Landers, R. G., and Hilmas, G. E., "Freeze-form Extrusion Fabrication of Functionally Graded Materials," *Journal of Manufacturing Technology-CIRP Annals*, Vol. 61, No. 1, 2012, pp.

[35]Schmidt, E. W., *Hydrazine and Its Derivatives: Preparation, Properties, Applications*, Wiley-Interscience, 2001.

[36]Sutton, D., "Hydrazine Thrusters for Space Applications," *Journal of the British Interplanetary Society*, Vol. 25, No. 1972, pp. 537-551.

[37]Englert, G. W., and Kochendorfer, F. D., "Estimated Performance of Radial-Flow Exit Nozzles for Air in Chemical Equilibrium," Rept. 1-5-59E, 1959.

[38]Humble, R. W., Henry, G. N., and Larson, W. J., *Space Propulsion Analysis and Design*, McGraw-Hill, 1995.

[39]Polzin, K. A., and Choueiri, E. Y., "Performance Optimization Criteria for Pulsed Inductive Plasma Acceleration," *IEEE Transactions on Plasma Science*, Vol. 34, No. 3, 2006, pp. 945-953.

[40]Polzin, K. A., Reneau, J. P., and Sankaran, K., "Incorporation of and Energy Equation into a Pulsed Inductive Thruster Performance Model," *32nd Inernational Electric Propulsion Conference*, IEPC-2011-181, 2011.

[41]Boyd, W. K., Berry, W. E., White, E. L., "Compatibility of Materials With Rocket Propellants and Oxidizers," United States Air Force Research and Technology Division, Rept. DMIC Memorandum 201, 1965.

[42]Hofer, R. R., Randolph, T. M., "Mass and Cost Model for Selecting Thruster Size in Electric Propulsion Systems," *Journal of Propulsion and Power*, Vol. 29, No. 1, 2013, pp. 166-177.

[43]Polzin, K. A., Rose, M. F., Miller, R., Best, S., Owens, T., and Dankanich, J., "Design of a Low-Energy FARAD Thruster," *43rd AIAA/ASME/SAE/ASEE Joint Propulsion Conference & Exhibit*, AIAA Paper 2007-5257, 2007.

[44]Dankanich, J. W., and Polzin, K. A., "Mission Assessment of the Faraday Accelerator with Radio-frequency Assisted Discharge (FARAD)," *44th AIAA/ASME/SAE/ASEE Joint Propulsion Conference & Exhibit*, AIAA Paper 2008-4517, 2008.

[45]Hallock, A. K., and Polzin, K. A., "Computational Validation of a Two-dimensional Semi-empirical Model for Inductive Coupling in a Conical Pulsed Inductive Plasma Thruster," *Joint Army-Navy-NASA-Air Force (JANNAF) 8th MSS/6th LPS/5th SPS Meeting*, JANNAF-2011-2197, 2011.